ENCIT 2018

ABCM Associação Brasileira de Engenharia e Ciências Mecânicas

17th Brazilian Congress of Thermal Sciences and Engineering
November 25th-28th, 2018, Águas de Lindóia, SP, Brazil

ENCIT-2018-0717
A STEADY-STATE MODEL TO PREDICT THE PERFORMANCE OF RECIPROCATING COMPRESSORS IN HOUSEHOLD REFRIGERATORS

Lucas C. LAZZARIS
Marco C. DINIZ
Cesar J. DESCHAMPS
POLO Research Laboratories for Emerging Technologies in Cooling and Thermophysics
Federal University of Santa Catarina
Florianopolis, SC, Brazil
deschamps@polo.ufsc.br

Abstract. *The performance of reciprocating compressors is usually evaluated under fixed operating conditions defined in standards. However, their actual operating condition depends on the interaction with the other components of the refrigeration system. This paper presents a simulation model developed to characterize the performance of reciprocating compressors under typical conditions of household refrigerators. The simulation model is based on simultaneous solution of three sub models for the following processes: (i) compression cycle inside the cylinder, (ii) heat exchange between the internal components of the compressor, (iii) heat exchange in the remaining components of the refrigeration system. The model was validated by comparing predictions and experimental data of mass flow rate, energy consumption and evaporating and condensing temperatures of a refrigeration system in different operating conditions. After being validated, the model was used to simulate the effect of different compressor designs on the efficiency of the whole refrigeration system.*

Keywords: *Reciprocating Compressor, Household Refrigerator, Numerical Model*

1. Introduction

About 1.4 billion household refrigerators and freezers are in use worldwide (Barthel and Götz, 2012) and the vast majority of these appliances employ the vapor compression refrigeration cycle. Naturally, the performance of the refrigeration loop depends not only on the efficiency of each of its components, but also on the manner they interact with each other.

In household refrigerators, a necessary feature from the refrigeration system is the ability to provide higher cooling capacities than thermal load under typical operating conditions. Two main aspects justify this requirement. First, during the refrigerator pulldown - in which the refrigeration system must reduce the temperature of the refrigerated compartment from a value close to ambient temperature to the desired levels - the compressor operates under severe operating conditions and a considerable cooling capacity is required to reduce the pulldown time. Furthermore, when in typical operating conditions, the refrigeration system must be able to maintain the temperature of the refrigerated compartments in the desired levels even if there is an increase of the thermal load caused by events such as door openings, warm food and drink refill.

In typical operating conditions, due to the excess of cooling capacity, the compressor operates in part load, i.e, there are periods in which the compressor is either operating (on) or not operating (off), giving rise to the so-called cycling operating conditions. In contrast to what occurs during the pulldown, in a typical cycling operation of the refrigerator the time to reach a stabilized operating condition is short.

The cycling operating conditions of household refrigerators have been the focus of many studies, either through experimental investigation (Björk and Palm, 2006; Diniz *et al.*, 2018b) or simulation models (Janssen *et al.*, 1992; Hermes and Melo, 2008; Hermes *et al.*, 2009; Borges *et al.*, 2011). Despite the physical insight allowed by experimentation, simulation models often offer more flexibility and allow for parametric analyses. In this context, Hermes *et al.* (2009) developed a steady-state simulation model for a refrigeration system to predict runtime ratio and energy consumption of a household refrigerator operating under typical cycling conditions. Lumped steady-state approaches were applied to the refrigerant flow in the heat exchangers, while the effects of the capillary tube and refrigerant charge were characterized by fixed degrees of subcooling and superheating. Since the focus was not on the compressor, the authors estimated the mass flow rate and power consumption by using maps for the volumetric and isentropic efficiencies.

This paper presents a simulation model developed to characterize the performance of reciprocating compressors under typical conditions of household refrigerators. The model is based on the approach put forward by Hermes *et al.* (2009) but employs a detailed modeling of the compressor. The complete model consists of three sub models: one to predict the

compression cycle in the compression chamber, other to calculate the temperature of the compressor components, and the last one to predict the operating condition by solving the remaining components of the refrigeration system. Some input data required for the model were obtained from measurements, which were also used to validate the model predictions.

2. Simulation Model

The complete simulation model is formed by three sub models. The model is solved in an iterative manner until convergence is achieved. The next sections describe the mathematical formulation of each sub model.

2.1 Compressor Modeling

The compression cycle model follows a transient lumped formulation for the compression chamber. The model is based on four groups of equations (Todescat *et al.*, 1992). The first one is used to determine the volume occupied by the refrigerant inside the compression chamber. The second group of equations is composed by the conservation equations of the compressor chamber to determinate the refrigerant temperature and pressure. The mass conservation equation is given by Equation 1:

$$\frac{dm_{cc}}{dt} = \dot{m}_{sv} - \dot{m}_{sv,b} - \dot{m}_{dv} + \dot{m}_{dv,b} - \dot{m}_{pc} \tag{1}$$

where $\dot{m}$ is the instantaneous mass flow rate through control surface, the subscripts *sv*, *dv*, and *b* indicate the suction and discharge valves and backflow in both cases, respectively. While the subscripts *pc* and *cc* indicate leakage through the piston cylinder gap and compression chamber, respectively. As the volume and refrigerant mass are known, it is possible to characterize the refrigerant instantaneous density.

By applying the energy conservation equation inside the compression chamber it is possible to determinate the instantaneous refrigerant temperature:

$$\frac{dT_{cc}}{dt} = A - BT_{cc} \tag{2}$$

where:

$$A = \frac{1}{m_{cc}c_v}\left[\hbar A_w T_w - h_{cc}\frac{dm_{cc}}{dt} + \dot{m}_{sv}h_{sc} - \dot{m}_{sv,b}h_{cc} - \dot{m}_{dv}h_{cc} + \dot{m}_{dv,b}h_{dc} - \dot{m}_{pc}h_{cc}\right] \tag{3}$$

$$B = \frac{1}{m_{cc}c_v}\left[\hbar A_w + \left.\frac{\partial p_{cc}}{\partial T_{cc}}\right|_v \frac{d\forall_{cc}}{dt} - \left.\frac{\partial p_{cc}}{\partial T_{cc}}\right|_v v_{cc}\frac{dm_{cc}}{dt}\right] \tag{4}$$

In the above equations $\hbar$ is the convective heat transfer coefficient calculated using the correlation proposed by Annnad (1963). The temperatures from suction chamber (T_{sc}), discharge chamber (T_{dc}) and cylinder wall (T_w) are obtained via compressor thermal model, which will be described shortly. Two geometric parameters are present: the heat exchange area (A_w) and the compression chamber volume ($\forall_{cc}$). Knowing the density and the temperature calculated with Equation 2 it is possible to determinate the instantaneous refrigerant pressure via state equation.

The third group of equations is required to characterize the dynamics of the suction and discharge valves. A one degree-of-freedom mass-spring model is employed. The concept of effective force area is utilized to determinate the force acting on the valve.

Finally, the fourth group of equations calculates the mass flow rates that cross the control volume surfaces. The concept of effective flow areas is utilized to correct the theoretical value calculated using a model for the isentropic flow through a convergent nozzle. Both effective force and effective flow areas were previously obtained through CFD simulations. Mass leakage through the piston cylinder gap is estimated with a model for a fully developed laminar Couette-Poiseuille flow (Ferreira and Lilie, 1984).

In this work, pressure pulsations in the suction and discharge mufflers are calculated by solving a 1-D numerical model for the mufflers, as proposed by Deschamps *et al.* (2002).

Some parameters of the compression cycle model are inputs to the other two sub models: the electrical power consumption ($\dot{W}_e$), the indicated power ($\dot{W}_i$), mechanical losses ($\dot{Q}_b$), the discharge line temperature (T_{dl}) and mass flow rates. The mechanical losses and the electrical efficiency (η_e) were specified based on experimental data obtained for the compressor under analysis. As shown by Equations 1 and 2, the model for the compression chamber adopts a transient formulation. However, since the compressor thermal model and the model for the remaining components of the system

predict steady state conditions, and the compression cycle time scale is considerably smaller than that of the other components, the results must be averaged through a compression cycle. Table 1 shows the calculations needed to integrate the instantaneous parameters over time. In Table 1 f is the compressor speed and the subscripts dl, l and s refer to discharge line, leakage and suction, respectively.

Parameter	Calculation
$\dot{W}_i$	$f \oint p_{cc} d\forall_{cc}$
$\dot{m}_i$	$f \oint \dot{m}_i dt$, where i represents a control surface
T_{dl}	$\frac{1}{m_{dv}} \oint \dot{m}_{dv} T_{cc} dt$
$\dot{Q}_{mot}$	$(\dot{W}_i + \dot{Q}_b)(1 - 1/\eta_e)$

Table 1: Integration of the compression cycle model parameters

To calculate the temperature of the compressor components, steady state energy balances were applied to a group of pre-determined control volumes, generating a thermal network in which the control volumes interact through mass flow rates and thermal resistances (Diniz *et al.*, 2018a). The thermal resistances were modeled using the concept of global heat conductances, which were determined by adjusting the model to measurements of temperature distribution obtained in a calorimeter for operating conditions corresponding to evaporating and condensing temperatures of $-25.8\,^{\circ}\mathrm{C}$ and $46.6\,^{\circ}\mathrm{C}$, respectively, and ambient temperature of $32\,^{\circ}\mathrm{C}$.

Of special interest when solving the thermal model are the temperature in the suction chamber, cylinder and discharge chamber, which are used as input data for the compression cycle model, as well as the discharge line temperature, which is used as input data for the condenser model.

2.2 Modeling of Remaining System Components

The refrigeration system of a household refrigerator is composed by five main components: compressor, condenser, capillary tube, evaporator and suction line. A heat exchanger involving the capillary tube and the compressor suction line is commonly applied to increase cooling capacity and prevent liquid slug within the compressor. The compressor model was presented in section 2.1 This section presents the energy balances that are applied to the refrigerant flow within the remaining system components. The energy balance in the condenser is given by:

$$\dot{m}_c h_{dl} = \dot{m}_c h_{cd,o} + \dot{Q}_c \tag{5}$$

where $\dot{m}_c$ is the average compressor mass flow and the subscripts *i* and *o* refer to inlet and outlet. The heat loss between condenser and external environment (Q_c) can be calculated by using the concept of global heat conductances (UAs), as shown in Equation 6.

$$\dot{Q}_c = UA_{cd}(T_{cd} - T_{amb}) \tag{6}$$

For the evaporator, a similar energy balance is applied:

$$\dot{m}_c h_{ev,i} + \dot{Q}_e = \dot{m}_c h_{ev,o} \tag{7}$$

$$\dot{Q}_e = UA_{ev}(T_{fz} - T_{ev}) \tag{8}$$

where T_{fz} is the freezer temperature, subscripts ev and cd indicate evaporator and condenser, respectively. The capillary tube and suction line models are included in the internal heat exchanger model, whose energy balance is given by:

$$\dot{m}_c h_{ev,o} + \dot{m}_c h_{cd,o} = \dot{m}_c h_{ev,in} + \dot{m}_c h_{sl} \tag{9}$$

where the compressor suction line temperature, T_{sl}, is considered equal to ambient temperature. It is still necessary to provide fixed values of refrigerant subcooling and superheating at the condenser and evaporator outlets, respectively. This

procedure eliminates the necessity of a model to calculate the mass flow rate through the capillary tube and the prescription of refrigerant charge (Borges *et al.*, 2011).

$$T_{ev,o} = T_{ev,i} + \Delta T_{sup} \tag{10}$$

$$T_{vd,o} = T_{cd,i} - \Delta T_{sub} \tag{11}$$

In order to obtain the global heat conductances UA_{ev} and UA_{cd} the model was adjusted the operating condition (Diniz *et al.*, 2018a) defined by the evaporating and condensing temperatures used to obtain the compressor UAs. The parameters of interest from this model are the evaporating and condensing temperatures, which are used in the compression cycle model.

2.3 Solution Procedure

The solution procedure is based on exchange of information between the previously discussed sub models and it is solved through the Newton-Raphson method. First, the compression cycle model is called with initial values for the variables and operating conditions set, then the compressor thermal model is calculated and finally the models for the remaining components of the system, closing the iterative loop. Figure 1 presents the flowchart of this iterative process.

Since the sub models require input from each other, convergence must be verified after each iteration between the three sub models. In the present solution procedure, the simulation was considered converged if the average compressor discharge temperature varied less than $0.1\,^{\circ}\mathrm{C}$ between two iterations.

3. Results and Discussion

The predictions of the model were compared to measurements obtained by Diniz *et al.* (2018b). The authors tested a one door household refrigerator in a climate chamber under three different ambient temperatures (T_{amb}): 32.0, 25.0 and $16.0\,^{\circ}\mathrm{C}$. For each ambient temperature there were multiple freezer temperatures (T_{fz}). Table 2 shows the freezer temperatures for each condition, i.e, the test condition 32C refers to T_{amb}/T_{fz} = 32.0/$-17.7\,^{\circ}\mathrm{C}$.

Figure 2 presents the simulated results of evaporating and condensing temperatures, energy consumption and *RTR* for different *reservoirs* conditions.

T_{amb} [°C]	A	B	C
32	-9.3	-14.4	-17.7
25	-9.2	-14.0	-17.3
16	-	-13.1	-17.0

Table 2: Experimental T_{fz} [°C]

For this simplified steady state model, the *RTR* is determined by the ratio of the system thermal load ($\dot{Q}_l$) to the cooling capacity ($\dot{Q}_e$), represented by Equation 12. The system energy consumption ($\dot{E}$) can be estimated by multiplying the *RTR* by the steady state compressor power consumption ($\dot{W}_e$), as shown in Equation 13 (Hermes *et al.*, 2009).

$$RTR = \frac{\dot{Q}_l}{\dot{Q}_e} \tag{12}$$

$$\dot{E} = \dot{W}_e RTR \tag{13}$$

The thermal load is calculated by using the global heat conductance between the external environment and the freezer ($UA_{compart}$). It is worth noting that in this work the thermal load is a post-processing variable and does not affect the steady state evaporating and condensing temperatures, although a real system must have $\dot{Q}_e > \dot{Q}_l$.

$$\dot{Q}_l = UA_{compart}(T_{amb} - T_{fz}) \tag{14}$$

The comparison between experimental and numerical results in the different operating conditions shows good agreement, especially for lower freezer temperatures ($-17\,^{\circ}\mathrm{C}$). This can be explained by looking at the run time ratio (*RTR*)

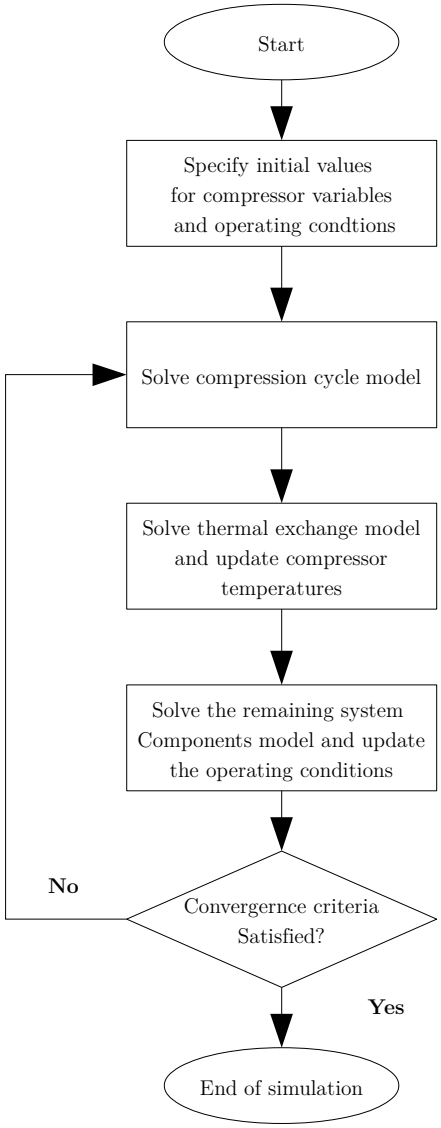

Figure 1: Flowchart of the solution procedure

results. This parameter indicates the percentage of the time in which the compressor is operating. Therefore, lower run time ratios have bigger effects of the system start-up transients, phenomena that the simplified steady state model cannot represent. In a real system, the instantaneous operating condition changes throughout the on-period, which induces time dependent variations in the cooling capacity and power consumption, which are not predicted by the model presented in this work. The model was calibrated at the condition 32C and it also loses accuracy as the T_{fz} increases. The operating conditions errors were in a range of ± 1.6 and $\pm 2.4\,^{\circ}\mathrm{C}$ for T_{ev} and T_{cd}, respectively.

Similarly as seen before for the operating conditions, for lower run time ratios the numerical model is able to predict the RTR and system energy consumption. The prediction for energy consumption for the highest RTR condition (32C) shows a deviation of 4.5%, and for longer off periods the deviation reaches 12.0%. The RTR show deviations in the range of 4.5%.

3.1 Parametric Analyses

The model can be used in a parametric analysis to evaluate the effect of compressor design parameters on the performance of the system. An advantage of this model over conventional compressor modeling approaches is the ability of predicting the performance of the entire refrigeration system and not only of the isolated compressor under calorimeter operating conditions.

A first parameter of interest is the clearance volume, which is required due to reliability issues. After the discharge process, part of the refrigerant is confined in this volume and expanded before the opening of the suction valve, thus

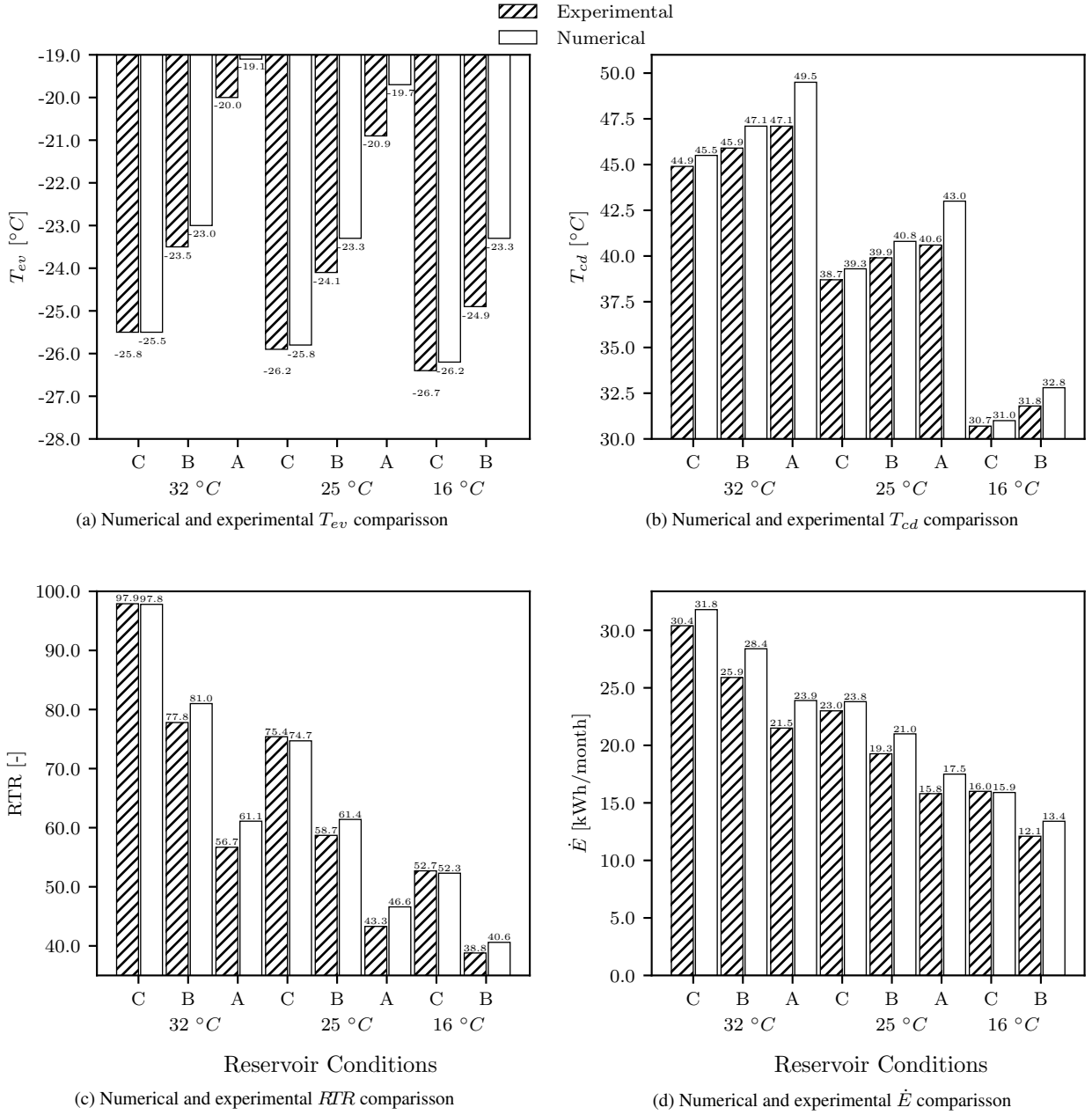

(a) Numerical and experimental T_{ev} comparisson

(b) Numerical and experimental T_{cd} comparisson

(c) Numerical and experimental *RTR* comparisson

(d) Numerical and experimental $\dot{E}$ comparisson

Figure 2: Measured and simulated results for different *reservoir* conditions

reducing the total amount of refrigerant admitted into the compression chamber. Besides the analyses that consider the compressor interacting with the system, the model can also be used to simulate the compressor under prescribed evaporating and condensing temperatures. Table 3a presents the results expected for the same compressor presented in the validation under calorimeter operating conditions T_{ev}/T_{cd} = −25.8/46.6 °C at 2949 RPM. The effect of varying the clearance volume, from -20 % to +20 % of its standard value, S, is analyzed. Table 3b presents the same analysis, but in this case considering the compressor interaction with the system under condition 32C. Table 4 presents the resulting operating conditions in the refrigerator, besides the main performance parameters.

When the clearance volume is reduced under the calorimeter conditions, the model predicts a slight increase of the coefficient of performance (*COP*). The same analyses conducted when the compressor is operating in a refrigeration system shows that the *COP* is less sensitive to changes in the compressor clearance volume. In this case, the decrease in the clearance volume increases compressor cooling capacity, which decreases the evaporating temperature and increases the condensing temperature, shown by Table 4. The decrease of the evaporating, or the increase of the condensing temperature cause a higher temperature difference between each heat exchanger and its respective *reservoir*, thus increasing the external thermodynamic irreversibilities. A second effect is the change in *RTR*, since a higher mass flow ratio results

Case	$\dot{W}_e$ [W]	$\dot{Q}_e$ [W]	COP
-20%	45.9	80.2	1.75
-10%	45.2	78.2	1.73
S	44.3	76.1	1.72
+10%	43.5	73.6	1.70
+20%	42.5	71.6	1.68

(a) Expected calorimeter results (-25.8/46.6 °C)

Case	$\dot{W}_e$ [W]	$\dot{Q}_e$ [W]	COP
-20%	47.1	81.0	1.72
-10%	46.5	79.6	1.72
S	45.7	78.3	1.71
+10%	45.0	76.9	1.71
+20%	44.2	75.6	1.71

(b) Expected system results (condition 32C)

Table 3: Clearance volume analyses

in a lower operating time of the compressor.

Case	T_{ev} [°C]	T_{cd} [°C]	$\dot{W}_e$ [W]	RTR [-]	$\dot{E}$ [kW h/month]
-20%	-25.1	46.2	47.1	91.4	31.0
-10%	-25.0	46.0	46.5	93.0	31.1
S	-24.9	45.8	45.7	94.5	31.1
+10%	-24.8	45.5	45.0	96.3	31.2
+20%	-24.7	45.3	44.2	97.9	31.2

Table 4: Operating conditions expected in a refrigeration system

The second parametric analysis is related to heat transfer inside the compressor. Suction gas superheating occurs as refrigerant flows from the compressor suction line to the suction chamber, decreasing the compressor performance. Therefore, thermal insulation in the suction system was investigated as an alternative to reduce superheating. The effect of thermal insulation was predicted for operating conditions of calorimeter and refrigeration system by varying the heat conductance between the suction muffler and the internal compressor environment in the range of $\pm 50\%$. The results are shown in Table 5.

Case	$\dot{W}_e$ [W]	$\dot{Q}_e$ [W]	COP
-50%	44.5	76.8	1.73
-25%	44.4	76.4	1.72
S	44.3	76.1	1.72
+25%	44.3	75.9	1.71
+50%	44.2	75.7	1.71

(a) Expected calorimeter results (-25.8/46.6 °C)

Case	$\dot{W}_e$ [W]	$\dot{Q}_e$ [W]	COP
-50%	45.8	78.6	1.71
-25%	45.8	78.5	1.71
S	45.7	78.3	1.71
+25%	45.7	78.1	1.71
+50%	45.7	78.0	1.71

(b) Expected system results (condition 32C)

Table 5: Suction heat exchange analyses

In calorimeter conditions, the model predicts a slight increase in compressor COP since the insulation of the suction system increases the cooling capacity more than it increases the power consumption. As can be seen in Tables 5b and 6, the insulation of the suction system virtually does not effect the COP when the system interaction is considered. This occurs because the temperature differences between both the evaporator and condenser and their respective *reservoir* slightly increases, in spite of a reduction of inefficiencies in the suction system.

Similarly to the analysis of the clearance volume, an increase of mass flow rate tends to increase the difference between the evaporating and condensing temperatures and those of their *reservoirs*, increasing irreversibilities. This aspect makes the design of compressors more difficult, since a common method to test the compressor performance is via experimentation in calorimeter and, not in the refrigerator. A calorimeter test cannot characterize the changes in the operating conditions that occur in the refrigeration system as a consequence of design modification.

The third analysis is related to changes in the compressor speed. Variable capacity compressors (VCCs) adopt frequency inverters to vary the compressor speed, in order to match the instantaneous cooling capacity to the thermal load. In the present analysis, the compressor speed was varied from 1200 to 4500 RPM. The results are shown in Table 7.

The simulations with RTR higher than 100 indicate that the prescribed freezer temperature cannot be reached because the compressor is not able to supply the cooling capacity equal or greater than the thermal load. However, since the RTR for this steady state model is just a post processing output, and an improved compartment thermal insulation (lower

Case	T_{ev} [°C]	T_{cd} [°C]	$\dot{W}_e$ [W]	*RTR* [-]	$\dot{E}$ [kW h/month]
-50%	-25.0	45.9	45.9	94.1	31.1
-25%	-24.9	45.8	46.8	94.3	31.1
S	-24.9	45.8	45.7	94.5	31.1
+25%	-24.8	45.7	45.7	94.8	31.2
+50%	-24.8	45.7	45.6	94.9	31.2

Table 6: Operating conditions expected in a refrigeration system

Case	T_{ev} [°C]	T_{cd} [°C]	$\dot{W}_e$ [W]	*RTR* [-]	$\dot{W}$ [kW h/month]	$\dot{Q}_e$ [W]	*COP*
1200	-21.8	39.7	23.5	176.4	29.9	42.0	1.78
1600	-22.7	41.7	28.6	141.0	29.1	52.5	1.80
2600	-24.3	44.6	40.6	103.5	30.2	71.5	1.76
3000	-25.0	45.9	46.4	93.5	31.2	79.1	1.70
3600	-25.5	47.3	53.4	85.4	32.8	86.6	1.62
4500	-26.0	48.6	61.4	79.7	32.2	92.8	1.51

Table 7: Operating conditions expected in a refrigeration system

$UA_{compart}$) would allow an *RTR* lower than 100. If the insulation is not changed, the lowest possible freezer temperatures for the 2600, 1600 and 1200 RPM cases are -17.0, -11.3 and $-8.0\,^{\circ}\mathrm{C}$, respectively.

Figures 3, 4 and 5 show the energy consumption and compressor overall efficiency for the conditions with freezer temperatures of -17.7, -16.0 and $-12.0\,^{\circ}\mathrm{C}$, respectively. The environment temperature was kept constant $T_{amb} = 32\,^{\circ}\mathrm{C}$ in all simulations. Figure 6 shows the normalized consumption for different freezer temperatures. The compressor overall efficiency (η_g) is given by:

$$\eta_g = \frac{\dot{W}_s}{\dot{W}_e} \tag{15}$$

where $\dot{W}_s$ is the compression power consumption for an isentropic process.

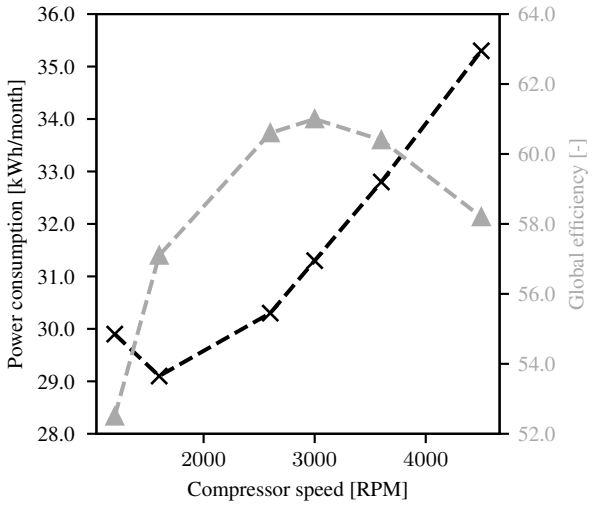

Figure 3: Impact of the compressor speed $T_{fz} = -17.7\,^{\circ}\mathrm{C}$

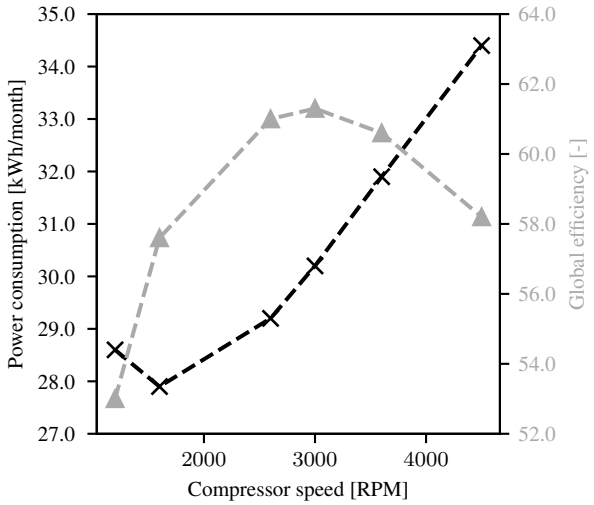

Figure 4: Impact of the compressor speed $T_{fz} = -16.0\,^{\circ}\mathrm{C}$

There is an optimum design point for the refrigeration system at 1600 RPM, which is not the best condition for the evaporator and condenser, since the lowest pressure ratio occurs for the 1200 RPM case.

The results demonstrate that the compressor speed that minimizes the system energy consumption is not the same that maximizes its overall efficiency. This shows that the optimized speed is a trade-off between the irreversibilites in the compressor and those in the heat exchangers. For instance, the case with T_{fz} $-17.7\,^{\circ}\mathrm{C}$ at 3000 RPM has the best

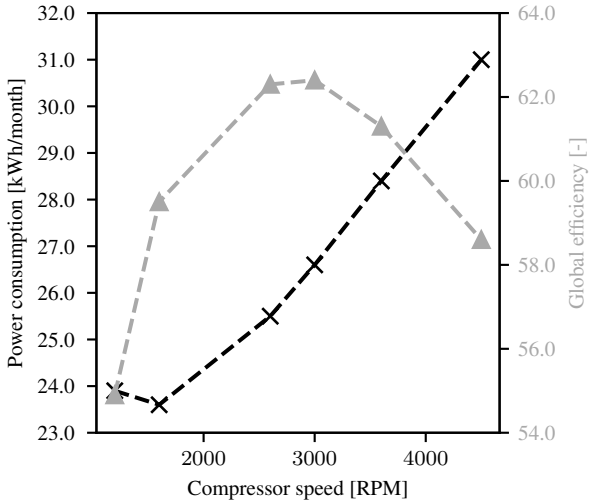

Figure 5: Impact of the compressor speed $T_{fz} = -12.0\,^{\circ}\mathrm{C}$

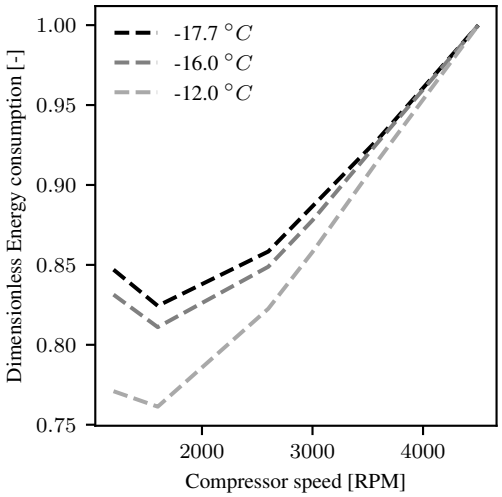

Figure 6: Impact of the compressor speed and the freezer temperature

overall efficiency for that freezer temperature, but the heat exchangers are far from their optimum point and the overall consumption is affected. It is also interesting to note that the increase of freezer temperature causes a slightly displacement of the optimum point towards lower compressor speeds.

4. Conclusion

This paper presented a simulation model developed to predict the performance of reciprocating compressors under typical operating conditions of household refrigerators. The model consists of three sub models, one for the compression cycle, one for the heat exchange between compressor components and a third model to determine the temperature of the remaining of the components of the refrigeration cycle. Some semi-empirical parameters required to the model were obtained by adjusting the model to available experimental data in one operating condition. Afterwards the model was validated by comparing measurements and predictions in different operating conditions, showing differences of 1.6 and $2.4\,^{\circ}\mathrm{C}$ for evaporating and condensing temperatures, respectively, 4.5% for RTR and maximum deviations of 12.0% for energy consumption. After the model validation, parametric analyses were carried out, in order to investigate the effects of compressor design modifications on its efficiency under calorimeter conditions and on the performance of the whole refrigeration system. The results reveal that the benefits of a more efficient compressor in a refrigeration system depend on the nature of the design change that increased its efficiency.

5. ACKNOWLEDGEMENTS

The present study was developed as part of a technical-scientific cooperation program between the Federal University of Santa Catarina and EMBRACO. The authors also acknowledge the support of EMBRAPII Unit POLO/UFSC and CAPES (Coordination for the Improvement of High Level Personnel).

6. REFERENCES

Annnad, W.J.D., 1963. "Heat Transfer In the Cylinders of Reciprocating Internal Combustion Engines". *Proceedings of the Institution of Mechanical Engineers*.

Barthel, C. and Götz, T., 2012. "The overall worldwide saving potential from domestic refrigerators and freezers". p. 40.

Björk, E. and Palm, B., 2006. "Refrigerant mass charge distribution in a domestic refrigerator, Part I: Transient conditions". *Applied Thermal Engineering*, Vol. 26, No. 8-9, pp. 829–837.

Borges, B.N., Hermes, C.J., Gonçalves, J.M. and Melo, C., 2011. "Transient simulation of household refrigerators: A semi-empirical quasi-steady approach". *Applied Energy*, Vol. 88, No. 3, pp. 748–754.

Deschamps, C.J., Possamai, F.C. and Pereira, E.L.L., 2002. "Numerical Simulation of Pulsating Flow in".

Diniz, M.C., Hermes, C.J.L. and Deschamps, C.J., 2018a. "Transient Simulation of Small-Capacity Reciprocating Compressors for On-Off Controlled Refrigerators". , No. 1991, pp. 1–10.

Diniz, M.C., Melo, C. and Deschamps, C.J., 2018b. "Experimental performance assessment of a hermetic reciprocating compressor operating in a household refrigerator under on-off cycling conditions". *International Journal of Refrigeration*, Vol. 88, pp. 587–598.

Ferreira, R. and Lilie, D., 1984. "Evaluation of the Leakage Through the Clearance Between Piston and Cylinder in Hermetic Compressors". *International Compressor Engineering Conference*.

Hermes, C.J. and Melo, C., 2008. "A first-principles simulation model for the start-up and cycling transients of household refrigerators". *International Journal of Refrigeration*, Vol. 31, No. 8, pp. 1341–1357.

Hermes, C.J., Melo, C., Knabben, F.T. and Gonçalves, J.M., 2009. "Prediction of the energy consumption of household refrigerators and freezers via steady-state simulation". *Applied Energy*, Vol. 86, No. 7-8, pp. 1311–1319.

Janssen, M.J.P., Wit, J.A.D. and Kuijpers, L.J.M., 1992. "Cycling losses in domestic appliances : an experimental and theoretical analysis". , No. 3.

Todescat, M.L., Fagotti, F., Prata, A.T. and Ferreira, R.T.D.S., 1992. "Thermal Energy Analysis in Reciprocating Hermetic Compressors". *Proceedings of the International Compressor Engineering Conference at Purdue*, pp. 1419–1428.

7. RESPONSIBILITY NOTICE

The authors are the only responsible for the printed material included in this paper.